Paper 200

©Civil-Comp Press, 2010
Proceedings of the Tenth International Conference
on Computational Structures Technology,
B.H.V. Topping, J.M. Adam, F.J. Pallarés,
R. Bru and M.L. Romero, (Editors),
Civil-Comp Press, Stirlingshire, Scotland

Refined Beam Models for Static and Dynamic Analysis of Wings and Rotor Blades

E. Carrera[1], E. Giorcelli[2], G. Mattiazzo[2] and M. Petrolo[1,3]
[1] Department of Aeronautic and Space Engineering
[2] Department of Mechanical Engineering
Politecnico di Torino, Italy
[3] Institut Jean Le Rond d'Alembert, UMR 7190 CNRS, Paris, France

Abstract

This paper presents the finite element analysis of slender thin-walled bodies by means of different finite element models. The beam formulation is given in the framework of the Carrera Unified Formulation, CUF, which considers the order of the theory, N, as a free parameter of the analysis. N is the order of the 1D displacement expansion. The displacement components are, in fact, expanded in terms of the cross-section coordinates, (x, z), by using a set of 1D generalized displacement variables. The refined kinematic models are based on Taylor-type polynomials. The finite element formulation is exploited in order to be able to face arbitrary cross-section geometries. FE's matrices are obtained in terms of a few fundamental nuclei which are formally independent of both N and the number of element nodes. A cubic (4 nodes) approximation along the beam axis, (y), is used. Structural analyses are conducted starting from classical beam theories, refined models are then introduced to evaluate non-classical effects. Aircraft wing and wind turbine blade models are analyzed. Static and dynamic analyses are conducted. It has mainly been concluded that the enhanced refined beam element, which has been formulated via CUF, is able to detect the so-called shell-like mechanical behaviors, that is, shell-like results can be obtained using higher-order beam elements. The shell-like capabilities include the detection of the local displacement field induced by a concentrated load, and natural modes characterized by the presence of waves along the cross-section contour.

Keywords: refined beam theories, finite element analysis, thin-walled structures, slender bodies, shell-like capabilities, wings, rotor blades.

1 Introduction

Lifting systems, LS's, are used in many engineering applications such as in engine turbines/compressors, helicopters, wind turbines, and aircrafts. A particular attention is herein given to aircraft wings and wind turbine rotor blades. The appropriate design of LS's consists of a number of important issues for structural analysts. Lifting systems appear as slender bodies in most of the applications, that is, the blades/wings length is predominant with respect to the cross-section dimensions. This geometrical feature permit us the adoption of the one-dimensional 1D approach for static, dynamic, and aeroelastic analyses.
Euler-Bernoulli's [1] and Timoshenko's [2, 3] theories are the classical models for beams made of isotropic materials. The former does not account for transverse shear effects on the cross-section deformations. The latter provides a model that, at best, foresees a constant shear deformation distribution on the cross-sections. Both theories yield better results for slender than for short beams. The static analysis requires refined beam elements for the proper detection of non-classical effects, such as the out-of-plane warping. As far as the free-vibration analysis is concerned, higher-order models are necessary for the detailed evaluation of high number modes. These issues are specially relevant for aircraft wings and rotor blades that require a detailed evaluation of the deformation fields and natural modes for the proper investigation of the aeroelastic phenomena (e.g. flutter, divergence, etc.).
There are several works concerning the construction of higher-order theories. Excellent reviews on these theories are those by Kapania and Raciti [4, 5]. Refined beam models for aerospace applications have been presented by Librescu [6] and Banerjee [9, 10]. A work on the effect of the shear deformation have been presented by Song and Waas [7]. The application of the asymptotical method to beam theories have been addressed by Yu and Hodges [8].
The finite element analysis is hereafter conducted in the framework of the Carrera Unified Formulation (CUF)[11, 12]. CUF was introduced during the last decade to implement higher-order shell theories. It has recently been extended to beam models [13, 14, 15, 16]. The main feature of CUF is represented by its hierarchical capabilities, in other words, in CUF the order of the formulation is considered as a free parameter of the analysis. Taylor-type polynomials are used to model the beam cross-section kinematic field. The finite element formulation is introduced to deal with arbitrary geometries, loading and boundary conditions. Four-node elements are used along the longitudinal axis of the beam. The Principle of Virtual Displacements (PVD) is exploited to compute the stiffness and mass matrices, and the loading vectors. Two different beam structures are analyzed: an aircraft wing and a wind turbine blade. Isotropic materials are adopted. Static and free-vibration analyses are conducted. This work is embedded in the Regione Piemonte project MICROCOST which is aimed to the development of small wind turbines for domestic use.

2 Description of Refined FE Beam Models

The adopted coordinate frame is presented in Fig. 1. The beam boundaries over y are

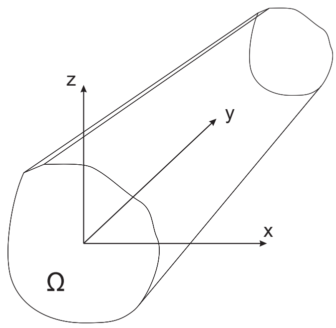

Figure 1: Coordinate frame of the beam model.

$0 \leq y \leq L$. The displacements vector is:

$$\mathbf{u}(x, y, z) = \left\{ \begin{array}{ccc} u_x & u_y & u_z \end{array} \right\}^T \tag{1}$$

Superscript "T" represents the transposition operator. The stress, $\boldsymbol{\sigma}$, and the strain, $\boldsymbol{\epsilon}$, are grouped as follows:

$$\begin{array}{ll} \boldsymbol{\sigma}_p = \left\{ \begin{array}{ccc} \sigma_{zz} & \sigma_{xx} & \sigma_{zx} \end{array} \right\}^T, & \boldsymbol{\epsilon}_p = \left\{ \begin{array}{ccc} \epsilon_{zz} & \epsilon_{xx} & \epsilon_{zx} \end{array} \right\}^T \\ \boldsymbol{\sigma}_n = \left\{ \begin{array}{ccc} \sigma_{zy} & \sigma_{xy} & \sigma_{yy} \end{array} \right\}^T, & \boldsymbol{\epsilon}_n = \left\{ \begin{array}{ccc} \epsilon_{zy} & \epsilon_{xy} & \epsilon_{yy} \end{array} \right\}^T \end{array} \tag{2}$$

Subscript "n" stands for terms laying on the cross-section, while "p" stands for terms laying on planes orthogonal to Ω. Linear strain-displacement relations are used:

$$\begin{array}{l} \boldsymbol{\epsilon}_p = \boldsymbol{D}_p \mathbf{u} \\ \boldsymbol{\epsilon}_n = \boldsymbol{D}_n \mathbf{u} = (\boldsymbol{D}_{n\Omega} + \boldsymbol{D}_{nz}) \mathbf{u} \end{array} \tag{3}$$

with:

$$\boldsymbol{D}_p = \begin{bmatrix} 0 & 0 & \frac{\partial}{\partial z} \\ \frac{\partial}{\partial x} & 0 & 0 \\ \frac{\partial}{\partial z} & 0 & \frac{\partial}{\partial x} \end{bmatrix}, \quad \boldsymbol{D}_{n\Omega} = \begin{bmatrix} 0 & 0 & 0 \\ 0 & \frac{\partial}{\partial x} & 0 \\ 0 & \frac{\partial}{\partial z} & 0 \end{bmatrix}, \quad \boldsymbol{D}_{ny} = \begin{bmatrix} 0 & \frac{\partial}{\partial y} & 0 \\ \frac{\partial}{\partial y} & 0 & 0 \\ 0 & 0 & \frac{\partial}{\partial y} \end{bmatrix} \tag{4}$$

The Hooke law is exploited:

$$\boldsymbol{\sigma} = \boldsymbol{C} \boldsymbol{\epsilon} \tag{5}$$

According to Eq.s 2, the previous equation becomes:

$$\begin{array}{l} \boldsymbol{\sigma}_p = \tilde{\boldsymbol{C}}_{pp} \boldsymbol{\epsilon}_p + \tilde{\boldsymbol{C}}_{pn} \boldsymbol{\epsilon}_n \\ \boldsymbol{\sigma}_n = \tilde{\boldsymbol{C}}_{np} \boldsymbol{\epsilon}_p + \tilde{\boldsymbol{C}}_{nn} \boldsymbol{\epsilon}_n \end{array} \tag{6}$$

In the case of isotropic material the matrices $\tilde{\boldsymbol{C}}_{pp}$, $\tilde{\boldsymbol{C}}_{nn}$, $\tilde{\boldsymbol{C}}_{pn}$ and $\tilde{\boldsymbol{C}}_{np}$ are:

$$\tilde{\boldsymbol{C}}_{pp} = \begin{bmatrix} \tilde{C}_{11} & \tilde{C}_{12} & 0 \\ \tilde{C}_{12} & \tilde{C}_{22} & 0 \\ 0 & 0 & \tilde{C}_{66} \end{bmatrix}, \quad \tilde{\boldsymbol{C}}_{nn} = \begin{bmatrix} \tilde{C}_{55} & 0 & 0 \\ 0 & \tilde{C}_{44} & 0 \\ 0 & 0 & \tilde{C}_{33} \end{bmatrix}, \quad \tilde{\boldsymbol{C}}_{pn} = \tilde{\boldsymbol{C}}_{np}^{T} = \begin{bmatrix} 0 & 0 & \tilde{C}_{13} \\ 0 & 0 & \tilde{C}_{23} \\ 0 & 0 & 0 \end{bmatrix} \tag{7}$$

For the sake of brevity, the dependence of the coefficients $[\tilde{C}]_{ij}$ versus Young's moduli and Poisson's ratio is not reported here. It can be found in Tsai [18] or Reddy [19].
In the framework of the Carrera Unified Formulation (CUF) [11, 12, 13, 14, 15, 16], the displacement field is assumed as an expansion in terms of generic functions, F_τ:

$$\mathbf{u} = F_\tau \mathbf{u}_\tau, \qquad \tau = 1, 2, ..., M \tag{8}$$

where F_τ are functions of the coordinates x and z on the cross-section. $\mathbf{u}_\tau$ is the displacement vector and M stands for the number of terms of the expansion. According to the Einstein notation, the repeated subscript τ indicates summation. Eq. (8) consists of a Maclaurin expansion that used as base the 2D polynomials $x^i\ y^j$, where i and j are positive integers. The maximum expansion order, N, is supposed to be 4. Table 1 presents M and F_τ as functions of N. For example, the second-order displacement field is:

$$\begin{aligned} u_x &= u_{x_1} + x\ u_{x_2} + z\ u_{x_3} + x^2\ u_{x_4} + xz\ u_{x_5} + z^2\ u_{x_6} \\ u_z &= u_{y_1} + x\ u_{y_2} + z\ u_{z_3} + x^2\ u_{z_4} + xz\ u_{z_5} + z^2\ u_{z_6} \\ u_z &= u_{z_1} + x\ u_{z_2} + z\ u_{z_3} + x^2\ u_{z_4} + xz\ u_{z_5} + z^2\ u_{z_6} \end{aligned} \tag{9}$$

N	M	F_τ
0	1	$F_1 = 1$
1	3	$F_2 = x \ \ F_3 = z$
2	6	$F_4 = x^2 \ \ F_5 = xz \ \ F_6 = z^2$
3	10	$F_7 = x^3 \ \ F_8 = x^2 z \ \ F_9 = xz^2 \ \ F_{10} = z^3$
...	...	...
N	$\frac{(N+1)(N+2)}{2}$	$F_{\frac{(N^2+N+2)}{2}} = x^N \ \ F_{\frac{(N^2+N+4)}{2}} = x^{N-1}z \ \ \ldots \ \ F_{\frac{N(N+3)}{2}} = xz^{N-1} \ \ F_{\frac{(N+1)(N+2)}{2}} = z^N$

Table 1: Mac Laurin's polynomials.

The Timoshenko beam model (TBM) can be obtained by acting on the F_τ expansion. Two conditions have to be imposed. 1) a first-order approximation kinematic field:

$$\begin{aligned} u_x &= u_{x_1} + x\ u_{x_2} + z\ u_{x_3} \\ u_y &= u_{y_1} + x\ u_{y_2} + z\ u_{y_3} \\ u_z &= u_{z_1} + x\ u_{z_2} + z\ u_{z_3} \end{aligned} \tag{10}$$

2) the displacement components u_x and u_z have to be constant above the cross-section:

$$u_{x_2} = u_{z_2} = u_{x_3} = u_{z_3} = 0 \tag{11}$$

The Euler-Bernoulli beam (EBBM) can be obtained through the penalization of ϵ_{xy} and ϵ_{zy}. This condition can be imposed by using a penalty value χ in the following constitutive equations:

$$\begin{aligned}\sigma_{xy} &= \chi\tilde{C}_{55}\epsilon_{xy} + \chi\tilde{C}_{45}\epsilon_{zy}\\ \sigma_{zy} &= \chi\tilde{C}_{45}\epsilon_{xy} + \chi\tilde{C}_{44}\epsilon_{zy}\end{aligned} \tag{12}$$

The classical theories and the first-order models require the assumption of opportunely reduced material stiffness coefficients to correct Poisson's locking (see Carrera and Brischetto [20, 21]). Unless differently specified, for classical and first-order models Poisson's locking is corrected according to Carrera and Giunta [13].
Introducing the shape functions, N_i, and the nodal displacement vector, $\mathbf{q}_{\tau i}$:

$$\mathbf{q} = \left\{ \begin{array}{ccc} q_{u_{x_{\tau i}}} & q_{u_{y_{\tau i}}} & q_{u_{z_{\tau i}}} \end{array} \right\}^T \tag{13}$$

The displacement vector becomes:

$$\mathbf{u}_\tau = N_i F_\tau \mathbf{q}_{\tau i} \tag{14}$$

For the sake of brevity, the shape functions are not reported here. They can be found in many books, for instance in [22]. Elements with 4 nodes (B4) are formulated, that is, a cubic approximation along the y axis is adopted. It has to be highlighted that, while the order of the beam model is related to the expansion on the cross-section, the number of nodes per each element is related to the approximation along the longitudinal axis. These two parameters are totally free and not related to each others. An N-order beam model is therefore a theory which exploits an N-order polynomial to describe the kinematics of the cross-section. The stiffness matrix of the elements and the external loadings, which are consistent with the model, are obtained via the Principle of Virtual Displacements:

$$\delta L_{int} = \int_V (\delta\boldsymbol{\epsilon}_p^T \boldsymbol{\sigma}_p + \delta\boldsymbol{\epsilon}_n^T \boldsymbol{\sigma}_n) dV = \delta L_{ext} \tag{15}$$

Where L_{int} stands for the strain energy, and L_{ext} is the work of the external loadings. δ stands for the virtual variation. The virtual variation of the strain energy is rewritten using Eq.s (3), (6) and (14), in a compact format it becomes:

$$\delta L_{int} = \delta\mathbf{q}_{\tau i}^T \mathbf{K}^{ij\tau s} \mathbf{q}_{sj} \tag{16}$$

Where $\mathbf{K}^{ij\tau s}$ is the stiffness matrix in the form of the fundamental nucleus. Its components are:

$$\begin{aligned} K_{xx}^{ij\tau s} = \; & \tilde{C}_{22}\int_\Omega F_{\tau,y}F_{s,y}d\Omega \int_l N_i N_j dy + \tilde{C}_{66}\int_\Omega F_{\tau,x}F_{s,x}d\Omega \int_l N_i N_j dy + \\ & \tilde{C}_{44}\int_\Omega F_\tau F_s d\Omega \int_l N_{i,z} N_{j,z} dy \\ K_{xy}^{ij\tau s} = \; & \tilde{C}_{23}\int_\Omega F_{\tau,y}F_s d\Omega \int_l N_i N_{j,z} dy + \tilde{C}_{44}\int_\Omega F_\tau F_{s,y} d\Omega \int_l N_{i,z} N_j dy \\ K_{xz}^{ij\tau s} = \; & \tilde{C}_{12}\int_\Omega F_{\tau,y}F_{s,x}d\Omega \int_l N_i N_j dy + \tilde{C}_{66}\int_\Omega F_{\tau,x}F_{s,y}d\Omega \int_l N_i N_j dy \end{aligned}$$

$$
\begin{aligned}
K_{yx}^{ij\tau s} = &\ \tilde{C}_{44}\int_{\Omega} F_{\tau,y}F_s d\Omega \int_l N_i N_{j,z} dy + \tilde{C}_{23}\int_{\Omega} F_{\tau}F_{s,y} d\Omega \int_l N_{i,z} N_j dy \\
K_{yy}^{ij\tau s} = &\ \tilde{C}_{55}\int_{\Omega} F_{\tau,x}F_{s,x} d\Omega \int_l N_i N_j dy + \tilde{C}_{44}\int_{\Omega} F_{\tau,y}F_{s,y} d\Omega \int_l N_i N_j dy + \\
&\ \tilde{C}_{33}\int_{\Omega} F_{\tau}F_s d\Omega \int_l N_{i,z} N_{j,z} dy \\
K_{yz}^{ij\tau s} = &\ \tilde{C}_{55}\int_{\Omega} F_{\tau,x}F_s d\Omega \int_l N_i N_{j,z} dy + \tilde{C}_{13}\int_{\Omega} F_{\tau}F_{s,x} d\Omega \int_l N_{i,z} N_j dy \\
K_{zx}^{ij\tau s} = &\ \tilde{C}_{12}\int_{\Omega} F_{\tau,x}F_{s,y} d\Omega \int_l N_i N_j dy + \tilde{C}_{66}\int_{\Omega} F_{\tau,y}F_{s,x} d\Omega \int_l N_i N_j dy \\
K_{zy}^{ij\tau s} = &\ \tilde{C}_{13}\int_{\Omega} F_{\tau,x}F_s d\Omega \int_l N_i N_{j,z} dy + \tilde{C}_{55}\int_{\Omega} F_{\tau}F_{s,x} d\Omega \int_l N_{i,z} N_j dy \\
K_{zz}^{ij\tau s} = &\ \tilde{C}_{11}\int_{\Omega} F_{\tau,x}F_{s,x} d\Omega \int_l N_i N_j dy + \tilde{C}_{66}\int_{\Omega} F_{\tau,x}F_{s,y} d\Omega \int_l N_i N_j dy + \\
&\ \tilde{C}_{55}\int_{\Omega} F_{\tau}F_s d\Omega \int_l N_{i,z} N_{j,z} dy
\end{aligned} \tag{17}
$$

The virtual variation of the work of the inertial loadings is:

$$
\delta L_{ine} = \int_V \rho \ddot{\boldsymbol{u}} \delta \boldsymbol{u}^T dV \tag{18}
$$

where ρ stands for the density of the material, and $\ddot{\boldsymbol{u}}$ is the acceleration vector. Eq. 18 is rewritten using Eq.s 3, and 14:

$$
\delta L_{ine} = \int_l \delta \mathbf{q}_{\tau i}^T N_i \left[\int_{\Omega} \rho (F_{\tau}\mathbf{I})(F_s \mathbf{I}) d\Omega \right] N_j \ddot{\boldsymbol{q}}_{sj} dz \tag{19}
$$

where $\ddot{\boldsymbol{q}}$ is the nodal acceleration vector. The last equation can be rewritten in the following compact manner:

$$
\delta L_{ine} = \delta \mathbf{q}_{\tau i}^T \mathbf{M}^{ij\tau s} \ddot{\boldsymbol{q}}_{sj} \tag{20}
$$

where $\mathbf{M}^{ij\tau s}$ is the mass matrix in the form of the fundamental nucleus. Its components are:

$$
\begin{gathered}
M_{xx}^{ij\tau s} = M_{yy}^{ij\tau s} = M_{zz}^{ij\tau s} = \rho \int_{\Omega} F_{\tau} F_s d\Omega \int_l N_i N_j dy \\
M_{xy}^{ij\tau s} = M_{xz}^{ij\tau s} = M_{yx}^{ij\tau s} = M_{yz}^{ij\tau s} = M_{zx}^{ij\tau s} = M_{zy}^{ij\tau s} = 0
\end{gathered} \tag{21}
$$

It should be noted that no assumptions on the approximation order have been done. It is therefore possible to obtain refined beam models without changing the formal expression of the nucleus components. This is the key-point of CUF which permits, with only nine FORTRAN statements, to implement any-order beam theories. The shear locking is corrected through the selective integration (see [22]). The undamped dynamic problem can be written as it follows:

$$
\boldsymbol{M}\ddot{\boldsymbol{a}} + \boldsymbol{K}\boldsymbol{a} = \boldsymbol{p} \tag{22}
$$

where $\boldsymbol{a}$ is the vector of the nodal unknowns and $\boldsymbol{p}$ is the loadings vector. Introducing harmonic solutions, it is possible to compute the natural frequencies, ω_i, for the homogenous case, by solving an eigenvalues problem:

$$(-\omega_i^2\mathbf{M} + \mathbf{K})\boldsymbol{a}_i = 0 \tag{23}$$

where $\boldsymbol{a}_i$ is the i-th eigenvector.

3 Results and Discussion

Two assessments are considered. The static analysis of a wing model is first assessed by means of a beam model. The results are compared with a solid finite element model. The free vibration analysis of a wind turbine rotor-blade is then done by using a shell model and comparing the results with experimental data.

3.1 Torsion of a wing model

A three-cell wing model is considered. Fig. 2 shows the geometric features of the cross-section. The NACA 2415 airfoil is used. The chord length, b, is assumed equal

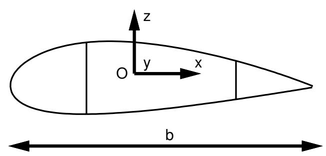

Figure 2: Wing cross-section.

to 1 [m]. The cells are obtained by inserting two beams along the span-wise direction at 25% and 75% of the chord. The span-to-chord ratio, L/b, is assumed to be equal to 5, that is, a moderately short structure is considered. An isotropic material is used. Young's modulus, E, is equal to 75 [GPa]. The Poisson ratio, ν, is equal to 0.33.
Static assessments of this model have been presented in [14], Fig. 3 shows the deformed free-tip cross-section due to a torsion loading. This result was obtained via a fourth-order ($N = 4$) model, the out-of-plane warping is well-detected. Unconventional wing geometries have been investigated in [17]. Fig.s 4 show a natural mode computed via a fourth-order beam model and compared with an MSC Nastran shell model. An excellent agreement between the two models has been found.

Higher than the forth-order models are herein considered. The torsion loading is obtained via the application of two opposite concentrated forces at the leading and

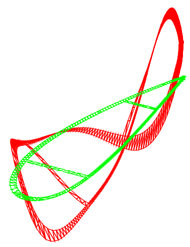

Figure 3: Torsion analysis of a wing model via a fourth-order beam model.

Figure 4: Natural mode of a joined-wing via CUF, $f = 47.512$ [Hz], and MSC Nastran Shell, $f = 47.118$ [Hz].

trailing edges. The forces are equal to ± 1000 [N]. Table 2 shows the value of displacement components at the trailing edge loading point for different beam models and the one computed via solid elements. The number of the degrees of freedom of each model is given in the second column.

The following conclusions hold.

1. Classical models are totally unable to evaluate the torsional behavior of the structure.

2. The refinement of the beam model offers significative improvements in the computation of the deformed configuration.

3. The computational cost of the higher-order 1D models is strongly smaller than in the case of solid element modelling.

Theory	DOF's	$u_x \times 10^5$ [m]	$u_z \times 10^3$ [m]
EBBM	155	0.0	0.0
TBM	155	0.0	0.0
N = 1	279	0.280	−0.074
N = 2	558	3.260	−0.681
N = 3	930	5.152	−0.818
N = 4	1395	5.620	−0.877
N = 5	1953	6.087	−0.944
N = 6	2604	6.477	−0.981
N = 7	3348	6.984	−1.029
N = 8	4185	7.231	−1.052
Solid	600000	6.926	−1.305

Table 2: u_z displacement at the trailing edge of the wing for different beam theories and comparison with a solid model.

3.2 Free vibrations analysis of a wind-turbine rotor blade

The MICROCOST rotor blade is herein investigated. The free vibration analysis is conducted via a shell model in MSC Nastran. The results are compared with those retrieved from experimental analyses. The rotor blades are shown in Fig. 5. A single

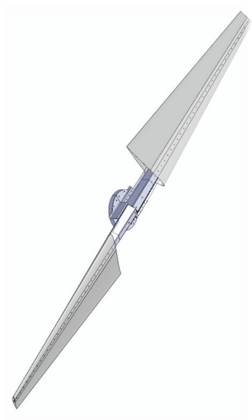

Figure 5: Rotor blades model.

blade is considered, it is modelled as a clamped-free structure composed by a main beam and a skin. The length of the blade is equal to 1 [m]. An isotropic material is used. Table 3 shows the comparison amongst the experimental natural frequencies and those computed via MSC Nastran. A good match is found especially for the first fundamental ones.

Mode	Experimental	MSC Nastran
I Bending	32	32
I Torsional	57	54
II Torsional	93	104
II Bending	169	146.5

Table 3: Natural frequencies [Hz] of the rotor blade.

4 Conclusions

Static and free vibration analyses of thin-walled aerospace structures have been presented in this paper. Higher-order theories have been systematically implemented by means of the Carrera Unified Formulation, CUF. According to CUF, the order of the model is assumed as a free parameter of the modelling by obtaining the element stiffness and mass matrices in compact forms, named fundamental nuclei, that do not depend on the theory approximation order. Elements based on classical theories, (Euler-Bernoulli and Timoshenko) have been derived as particular cases. Deformed configurations, natural frequencies, and vibration modes have been computed and compared with those from shell and solid models of commercial FE codes. The following main conclusions can be drawn.

1. CUF permits to deal in an unified manner with arbitrary cross-section geometries and thin-walled structures.

2. The use of higher-order theories allows us to overcome classical beam model limitations.

3. The comparison with shell and solid models has shown the shell capabilities of the refined beam theories in detecting the localized effects of concentrated loads and shell-like natural modes.

4. The computational effort requested by the present beam model is strongly smaller than those needed by shell and solid elements.

The use of the proposed beam model appears suitable to investigate the structural behavior of thin-walled structures such as the presented wind turbine blade.

Acknowledgments

The financial support from the Regione Piemonte project MICROCOST is gratefully acknowledged.

References

[1] L. Euler, “De curvis elasticis”, Lausanne and Geneva: Bousquet, 1744.

[2] S. P. Timoshenko, “On the corrections for shear of the differential equation for transverse vibrations of prismatic bars”, Philosophical Magazine, 41:744–746, 1921.

[3] S. P. Timoshenko, “On the transverse vibrations of bars of uniform cross section”, Philosophical Magazine, 43:125–131, 1922.

[4] K. Kapania and S. Raciti, “ Recent advances in analysis of laminated beams and plates, part I: Shear effects and buckling”, AIAA Journal, 27(7):923–935, 1989.

[5] K. Kapania and S. Raciti, “Recent advances in analysis of laminated beams and plates, part II: Vibrations and wave propagation”, AIAA Journal, 27(7):935–946, 1989.

[6] O. Song and L. Librescu, “Free vibration of anisotropic composite thin-walled beams of closed cross-section contour”, Journal of Sound and Vibration, 167(1):129–147, 1993.

[7] S. J. Song and A. M. Waas, “Effects of shear deformation on buckling and free vibration of laminated composite beams”, Composite Structures, 37(1):33–43, 1997.

[8] W. Yu and D. H. Hodges, “Generalized Timoshenko theory of the variational asymptotic beam sectional analysis”, Journal of the American Helicopter Society, 50(1):46–55, 2005.

[9] J. R. Banerjee and F. W. Williams, “Coupled bending-torsional dynamic stiffness matrix for Timoshenko beam elements”, Computers and Structures, 42(3):301–310, 1992.

[10] J. R. Banerjee, S. Guo, and Howson W. P., “Exact dynamic stiffness matrix of a bending-torsion coupled beam including warping”, Computers and Structures, 59(4):613–621, 1996.

[11] E. Carrera, “Theories and finite elements for multilayered, anisotropic, composite plates and shells”, Archives of Computational Methods in Engineering, 9(2):87–140, 2002.

[12] E. Carrera, “Theories and finite elements for multilayered plates and shells: a unified compact formulation with numerical assessment and benchmarking”, Archives of Computational Methods in Engineering, 10(3):216–296, 2003.

[13] E. Carrera and G. Giunta, “Refined beam theories based on Carrera’s unified formulation”, International Journal of Applied Mechanics, In Press.

[14] E. Carrera, G. Giunta, P. Nali, and M. Petrolo, “Refined beam elements with arbitrary cross-section geometries”, Computers and Structures, 88(5–6):283–293, 2010, DOI: 10.1016/j.compstruc.2009.11.002.

[15] E. Carrera, M. Petrolo, and P. Nali, “Unified formulation applied to free vibrations finite element analysis of beams with arbitrary section”, Shock and Vibrations, 17:1–18, 2010, DOI: 10.3233/SAV-2010-0528.

[16] E. Carrera and M. Petrolo, “On the effectiveness of higher-order terms in refined beam theories”, Journal of Applied Mechanics, In Press.

[17] E. Carrera, M. Petrolo, and A. Varello. "Advanced Beam Formulations for Free Vibration Analysis of Conventional and Joined Wings", Submitted.

[18] S. W. Tsai, "Composites Design", Dayton, Think Composites, 4th edition, 1988.

[19] J. N. Reddy, "Mechanics of laminated composite plates and shells. Theory and Analysis", CRC Press, 2^{nd} edition, 2004.

[20] E. Carrera and S. Brischetto, "Analysis of thickness locking in classical, refined and mixed multilayered plate theories", Composite Structures, 82(4):549–562, 2008.

[21] E. Carrera and S. Brischetto, "Analysis of thickness locking in classical, refined and mixed theories for layered shells", Composite Structures, 85(1):83–90, 2008.

[22] K.J. Bathe, "Finite element procedure", Prentice hall, 1996.